

The effects of genetic deletion of Macrophage migration inhibitory factor on the chronically hypoxic pulmonary circulation

Lili Li¹ , Maojia Xu¹, Simon C. Rowan¹ , Katherine Howell¹, Adam Russell-Hallinan¹, Seamas C. Donnelly², Paul McLoughlin^{1,*} and John A. Baugh^{1,*}

¹UCD Conway Institute for Biomolecular and Biomedical Research, University College Dublin, Dublin, Ireland; ²Department of Medicine, Tallaght University Hospital & Trinity College Dublin, Dublin, Ireland

Abstract

While it is well established that the haemodynamic cause of hypoxic pulmonary hypertension is increased pulmonary vascular resistance, the molecular pathogenesis of the increased resistance remains incompletely understood. Macrophage migration inhibitory factor is a pleiotropic cytokine with endogenous tautomerase enzymatic activity as well as both intracellular and extracellular signalling functions. In several diseases, macrophage migration inhibitory factor has pro-inflammatory roles that are dependent upon signalling through the cell surface receptors CD74, CXCR2 and CXCR4. Macrophage migration inhibitory factor expression is increased in animal models of hypoxic pulmonary hypertension and macrophage migration inhibitory factor tautomerase inhibitors, which block some of the functions of macrophage migration inhibitory factor, and have been shown to attenuate hypoxic pulmonary hypertension in mice and monocrotaline-induced pulmonary hypertension in rats. However, because of the multiple pathways through which it acts, the integrated actions of macrophage migration inhibitory factor during the development of hypoxic pulmonary hypertension were unclear. We report here that isolated lungs from adult macrophage migration inhibitory factor knockout (*MIF*^{-/-}) mice maintained in normoxic conditions showed greater acute hypoxic vasoconstriction than the lungs of wild type mice (*MIF*^{+/+}). Following exposure to hypoxia for three weeks, isolated lungs from *MIF*^{-/-} mice had significantly higher pulmonary vascular resistance than those from *MIF*^{+/+} mice. The major mechanism underlying the greater increase in pulmonary vascular resistance in the hypoxic *MIF*^{-/-} mice was reduction of the pulmonary vascular bed due to an impairment of the normal hypoxia-induced expansion of the alveolar capillary network. Taken together, these results demonstrate that macrophage migration inhibitory factor plays a central role in the development of the pulmonary vascular responses to chronic alveolar hypoxia.

Keywords

macrophage migration inhibitory factor, pulmonary vasoconstriction, pulmonary vascular resistance, pulmonary hypertension, alveolar capillary bed

Date received: 11 December 2019; accepted: 18 June 2020

Pulmonary Circulation 2020; 10(4) 1–13

DOI: 10.1177/2045894020941352

Introduction

Pulmonary hypertension (PH) is a disease of the pulmonary vasculature, characterised by sustained elevation of pulmonary vascular resistance (PVR) and pulmonary arterial pressure, which can ultimately lead to the development of right ventricular (RV) hypertrophy, RV failure and death.^{1,2}

*These authors contributed equally to this work.

Corresponding author:

John A. Baugh, UCD Conway Institute for Biomolecular and Biomedical Research, School of Medicine, University College Dublin, Belfield, Dublin, Ireland.

Email: john.baugh@ucd.ie



Creative Commons Non Commercial CC BY-NC: This article is distributed under the terms of the Creative Commons Attribution-NonCommercial 4.0 License (<http://creativecommons.org/licenses/by-nc/4.0/>) which permits non-commercial use, reproduction and distribution of the work without further permission provided the original work is attributed as specified on the SAGE and Open Access pages (<https://us.sagepub.com/en-us/nam/open-access-at-sage>).

© The Author(s) 2020.
Article reuse guidelines:
sagepub.com/journals-permissions
journals.sagepub.com/home/pul



Chronic hypoxia in healthy sea-level natives who move to high altitude frequently causes PH. This hypertension results from increased PVR as cardiac output and left atrial pressure are unchanged following acclimatization to hypoxia.³ Chronic alveolar hypoxia is also a significant contributor to the development of PH in chronic lung diseases.^{1,2,4-6} However, the molecular mechanisms leading to the increased vascular resistance that causes hypoxic pulmonary hypertension (HPH) remain to be fully elucidated.

Recently, it has been demonstrated that macrophage migration inhibitory factor (MIF), a hypoxia-responsive gene regulated by both hypoxia inducible factor (HIF)-1 and cyclic adenosine monophosphate response element binding protein (CREB) in hypoxia,⁷ may play a role in the development of PH. Increased serum MIF has been reported in pulmonary arterial hypertension, PH secondary to heart failure (with preserved ejection fraction) and PH complicating interstitial lung diseases.⁸ Inhibitors of the enzymatic tautomerase activity of MIF, ISO-1 and its analogue ISO-92, attenuate hypoxia-induced PH in mice and monocrotaline (MCT)-induced PH in rats.^{9,10} As there is no known physiological substrate for MIF tautomerase activity, it is suggested that these MIF enzymatic inhibitors attenuate PH via inhibition of the binding of MIF to one of its cell surface receptors CD74. This proposal is supported by *in vitro* data indicating that ISO-1 and its analogue ISO-92 block the interaction of MIF and CD74.¹¹⁻¹⁵ Furthermore, ISO-1 and antibody-based blockade of CD74 have been shown to have identical antihypertensive effects in MCT-induced PH suggesting that blockade of MIF action at this receptor is an important mechanism by which ISO-1 ameliorates the development of PH *in vivo*.¹⁰

However, MIF alters cellular functions by signalling through several different pathways. It binds to at least three distinct cell surface receptors: a CD74/44 complex, CXCR2 and CXCR4.¹⁶⁻¹⁸ In addition, MIF acts as an anti-oxidant, a protein chaperone and through its intra-cellular interaction with the c-Jun N-terminal activation domain-binding protein-1 (JAB-1).¹⁹⁻²² Finally, while MIF tautomerase inhibitors such as ISO-1 block some actions of MIF, it is unclear what the functional role of this endogenous enzymatic activity is *in vivo*.^{15,23,24}

Given that MIF acts via multiple signalling pathways, it is likely that this pleiotropic cytokine has functions in the chronically hypoxic pulmonary circulation that are not blocked by the previously described tautomerase inhibitors. Thus the integrated action of MIF in the development of the increased PVR induced by chronic alveolar hypoxia (i.e. the sum of the combined effects of all its signalling mechanisms) is unknown. In order to gain a clearer understanding of the integrated action of MIF in the chronically hypoxic lung, we examined the changes in PVR and structure in response to sustained exposure to hypoxia (21 days) in mice in which the MIF gene had been deleted (MIF knockout (*MIF*^{-/-}) mice) and compared these to wild-type (*MIF*^{+/+}) mice exposed to the same conditions.

Materials and methods

Animals

MIF^{-/-} mice were generously provided by Prof Jürgen Bernhagen (RWTH Aachen University, Germany) and the wild-type C57BL/6N mice (*MIF*^{+/+}) were purchased from Charles River. Heterozygous (*MIF*^{+/-}) mice were obtained from cross-breeding of *MIF*^{-/-} with *MIF*^{+/+} mice and the heterozygous mice were then paired for subsequent breeding to generate age-matched male mice *MIF*^{-/-} and wild-type mice. Genotype was confirmed by analysis of genomic DNA as previously described.²⁵ Mice were housed in climate controlled rooms under a 12 h light–12 h dark cycle, with *ad libitum* access to water and food. All animal procedures were approved by the University Ethics Committee and conducted under licence from the Department of Health and Children.

Chronic alveolar hypoxia

To determine the role of MIF in the development of the pulmonary vascular changes caused by chronic alveolar hypoxia, homozygous *MIF*^{-/-} male mice were compared to the litter matched *MIF*^{+/+} mice obtained during heterozygous breeding. Adult male specific pathogen free mice between 12 and 15 weeks old were used in this study. To induce HPH, animals were exposed to hypoxia (FiO₂, 0.10) for 21 days as previously described.^{26,27} Litter-matched animals were maintained in the same room under normoxic conditions for the same period of time. All subsequent analyses were conducted in a blinded fashion.

Isolated perfused mouse lung protocol

In order to study the effects of chronic hypoxia on PVR, we used the isolated ventilated perfused lung preparation. Pulmonary arterial pressure *in vivo* is affected by multiple factors in addition to the resistance of the vascular bed including changes in cardiac output, left atrial pressure, lung volume, airway pressure and reflex mechanisms. Use of the isolated lung allows maintenance of constant pulmonary flow, left atrial pressure and tidal volume and frequency so that changes in the pulmonary arterial pressure are directly related to changes in vascular resistance caused by hypoxia-induced alterations in the pulmonary vascular bed. All studies were conducted using a commercially available isolated perfused mouse lung apparatus (IL-1; Hugo Sachs Electronick-Harvard Apparatus, March, Germany), as previously described.^{27,28} Animals were anaesthetised (sodium pentobarbitone 70 mg.kg⁻¹ intra-peritoneal) and anti-coagulated using Heparin (1000 I.U./kg intra-peritoneal). A tracheal cannula was inserted via a tracheostomy and mechanical ventilation initiated (tidal volume 200 µl, rate 90–100 breaths/min, positive end-expiratory pressure (PEEP) 3 cmH₂O, 5% CO₂ in air). Mice were then killed by exsanguination and blood was collected for

determination of haematocrit. An incision was then made from the sternal notch to the xiphoid process and extended bilaterally along the inferior borders of the rib cage to the posterior abdominal wall. The diaphragm was incised and detached circumferentially to the midline of the posterior thoracic/abdominal wall. The thoracic cavity was opened via midline sternotomy, exposing the heart and lungs. The pulmonary artery (PA) and left atrium were cannulated in situ via the corresponding cardiac ventricles, and catheters were secured in place using 6-0 silk suture. The pulmonary circulation was perfused at constant flow (2 ml/min) with a non-pulsatile pump. Dulbecco's modified Eagle's medium (Sigma) was used as the perfusion buffer with Ficoll PM70 (Sigma) added to a final concentration of 4% (w/v) and the pH was adjusted to 7.4 with HCl. Perfusion buffer was freshly made for each experiment, and the temperature was maintained at 37°C within a water-jacketed perfusion chamber. The lungs were hyper-inflated once every 5 min in order to prevent the development of progressive atelectasis. Pulmonary artery (P_{PA}), left atrium (P_{LA}) and airway (P_{AW}) pressure were continuously recorded by high (vascular) pressure transducers (HSE P75 73-0020 type 379) and low differential pressure transducer (HSE MPX type 399/2), respectively, digitised and displayed using computer software (AcqKnowledge 3.8.2, Biopac Systems).

To examine acute hypoxic vasoconstriction, after stable normoxic PA pressure was established, the ventilation gas was changed to an hypoxic mixture (O_2 3%, CO_2 5%, balance N_2) for 10 min, by which time the increased PA pressure had stabilized in all lungs. Acute hypoxic vasoconstriction was assessed in two ways: first it was calculated as the difference between the PVR measured in normoxia immediately prior to the initiation of ventilation with the hypoxic gas, and the peak vascular resistance during the 10-min period of hypoxic ventilation (peak change). The second way in which acute hypoxic vasoconstriction was assessed was the difference between the PVR in normoxia immediately prior to switching to hypoxic gas and the steady state vascular resistance at the end of the 10-min period in hypoxia (steady state change).

The ventilating gas was then returned to the normoxic mix (5% CO_2 in air) for a further 10 min. For the groups treated with rho-kinase (ROCK) inhibitor (Y-27632), after the initial stable normoxic baseline PA pressure was established, Y-27632 (10^{-5} M, Merck Biosciences) was added to the perfusate and the pressure change was recorded for 20 min to ensure that PA pressure had again stabilized. After the hemodynamic measurements were complete, the hearts were separated from the lungs and the lungs were flash-frozen for later RNA and protein analysis.

The hearts were separated from the lungs, fixed by immersion in paraformaldehyde (4% w/v in normal saline) and used to determine the ratio of the right ventricle to the left ventricle plus septum (RV/LV + S) as previously described.²⁹ Briefly, the atria were removed at the level of the atrioventricular junction in the plane of the mitral and

tricuspid annuli (i.e. at the level of the openings of the tricuspid and mitral valves where the valve leaflets attach). The ventricles were then transected parallel to this plane, at a level one-third of the distance from the atrioventricular junction to the apex of the heart. The cross sectional areas of the cut surfaces of the right and left ventricles were determined by stereological analysis and the ratio of these two values was calculated and taken as the RV/LV + S for that heart.

Tissue preparation

Hypoxia-induced changes in pulmonary vascular structure were assessed in separate groups of $MIF^{+/+}$ and $MIF^{-/-}$ mice exposed to hypoxia or normoxia for three weeks. Mice were anaesthetised, anti-coagulated and then killed by exsanguination as previously described.²⁹ Normal saline solution was perfused through the pulmonary circulation until the lungs were uniformly white and the draining perfusate was clear. An incision was made at the apex of the left ventricle to allow free drainage. Then rho-kinase inhibitor (Y-27632, 10^{-5} M, Merck Biosciences) was added to the perfusate to inhibit ROCK activity and ensure complete relaxation of vasomotor tone.³⁰ The left lung was then perfused with defibrinated horse blood (Cruinn Diagnostics Ltd) via the PA by gradually increasing pressure from 5 cm to 30 cm and maintaining pressure at 30 cm for at least 15 min. The presence of erythrocytes in the vascular space facilitated identification of vessels within the pulmonary parenchyma, following the preparation of sections for microscopic examination. Once all the blood vessels had been filled, indicated by a uniformly red appearance of all lobes, the wound at the apex of the left ventricle was closed using a vascular clamp ensuring that pressure throughout the vasculature was uniform (30 cmH₂O) and the PA was then sealed using a ligature. The lungs were then inflated with fixative (2.5% w/v glutaraldehyde in sodium cacodylate buffer, 350 mOsm, Ph 7.40) via the trachea at a constant airway pressure (25 cmH₂O) for 30 min. The left main bronchus was occluded by a ligature at the hilum so that the volume of air spaces, airways and vessels remained constant and the left lung was separated and immersed in fixative overnight.

Left lung volumes were measured by water displacement 24 h after removal and the lung then processed for stereological quantification of the pulmonary vascular bed.³¹ Briefly, the lung was divided into multiple blocks (approximately $2 \times 2 \times 4$ mm); a systematic randomised sampling strategy was used to select a subset of blocks from glutaraldehyde-fixed left lungs for embedding in resin and preparation of isotropically uniform random semi-thin (1μ) sections for stereological analysis. This method of fixation and embedding prevents shrinkage, maintaining vascular dimension closer to their in vivo values than conventional wax embedding.²⁹ The semi-thin sections were stained with toluidine blue for microscopic examination.

Stereological quantification of vascular dimensions

The stereological analysis undertaken in this study conforms to the guidelines of the Joint Standards for Quantitative Assessment of Lung Structure, as defined by the American Thoracic Society and European Respiratory Society joint task force.³²

Random microscopic images of the lung sections were selected ($\times 20$ objectives, Olympus BX61 motorised microscope) using a semi-automated Computer-Assisted Stereological Toolbox system (Visiopharm integrator system, version 2.9.11.0; Olympus Denmark). These images were digitised (Olympus DP70 digital camera) and displayed on screen to allow stereological determination of the length density of the vessels within the gas exchange region of the lung (intra-acinar vessels), lumen diameter and wall thickness, and capillary endothelial surface area as previously described.^{26,27} Intra-acinar vessels were identified as those accompanying respiratory bronchioles or more distal airways and alveoli, which had a diameter $> 10 \mu\text{m}$ but $< 100 \mu\text{m}$. For assessment of capillary endothelial surface area, images of tissue were randomly selected from the tissue section at high magnification ($\times 100$ oil immersion objective, NA 1.4). All slides were identified by code so that the observer was blinded to the experimental conditions in which the mice had been housed.

Western blotting

Western blot analysis was performed using whole lung lysates that were lysed in radioimmunoprecipitation assay buffer supplemented with protease and phosphatase inhibitors (Roche). Tissue was homogenized by mechanical disruption (TissueRuptor, Qiagen). Total protein content was determined using the Bicinchonic Acid (BCA) assay (Pierce). Equal amounts of protein ($20 \mu\text{g}$) from each sample were loaded onto the gel and proteins were separated by SDS-PAGE and blotted using rabbit anti-MIF (1:1000 dilution, product TP234, lot 032415, Torrey Pines Biolabs), rabbit anti- β -tubulin (1:1000 dilution, product 2146, Cell Signaling) and Horse radish peroxidase (HRP) conjugated goat anti-rabbit secondary antibodies (1:2000 dilution, Cell Signaling). Densitometry was performed using ImageJ software normalized to the normoxic samples.

Cell culture

Primary human pulmonary microvascular endothelial cells (HPMECs) derived from a male donor (C-12281; PromoCell) were maintained in endothelial cell basal medium (BM) MV2 supplemented with 5% Fetal calf serum (FCS), ascorbic acid and hydrocortisone, together with the following growth factors: human epidermal growth factor, human fibroblast growth factor, insulin-like growth factor-1 and human vascular endothelial growth factor (VEGF), according to the manufacturer's recommendations. Cells were used for experiments between passages four and six.

Apoptosis

Apoptosis in HPMECs were examined using caspase 3/7 activity as an index. Caspase 3/7 activity (Caspase-Glo 3/7 Assay; Promega) assays were performed in a 96-well-plate 24 h after treatment with MIF according to the manufacturer's guide.

Statistical analysis

All statistics were carried out using IBM SPSS Statistics software. Results are expressed as mean and standard deviation of the mean (SD), while non-normally distributed data are presented as medians and interquartile range. For normally distributed data, statistical significance of differences between two group means was determined using t-tests. For non-normally distributed data, statistical significance was determined using the Mann-Whitney rank sum (unpaired). For four group designs, correction for multiple post hoc comparisons was made using the Holms-Sidak step-down procedure.³³ Values of $P < 0.05$ were accepted as statistically significant.

Results

Expression of MIF in mouse lung

As expected, MIF protein was undetectable in the lungs of $MIF^{-/-}$ mice (Supplemental Fig. 1). Expression of MIF protein was increased by hypoxia in the lung of $MIF^{+/+}$ mice in

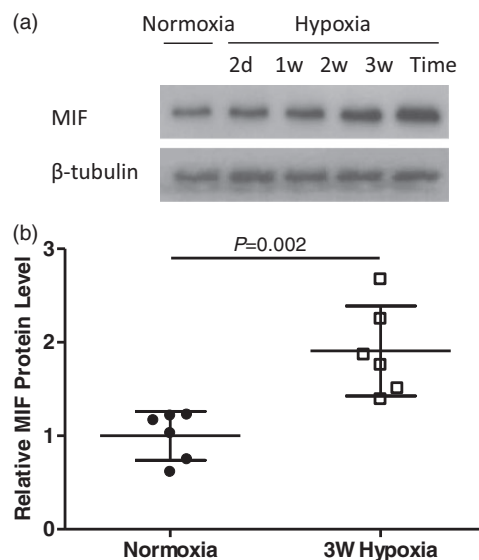


Fig. 1. MIF protein expression in $MIF^{+/+}$ mouse lung. (a) Representative images of western blots of MIF and β -tubulin protein expression. Mice were treated with hypoxic exposure for the time period as indicated. (b) Optical density analysis of western blots examining MIF expression in normoxic and three weeks hypoxic lungs of $MIF^{+/+}$ mice ($n = 6$). Values are expressed as mean (\pm SD) relative to mean normoxic value. MIF: Nacrophage migration inhibitory factor.

a time-dependent manner (Fig. 1a) and was significantly increased in the lungs of wild-type mice exposed to hypoxia for three weeks (Fig. 1b).

Acute hypoxic pulmonary vasoconstriction

When challenged with acute hypoxia (3% O₂ in the ventilating gas for 10 min), lungs from *MIF*^{+/+} mice showed an increase in PA pressure reflecting increased PVR, which peaked within minutes of the onset of hypoxia, followed by a decline to a lower value that stabilised before the end of the hypoxic period (Fig. 2a); the magnitude and pattern of the PA pressure response to hypoxia that we observed was similar to that reported by others in murine lungs perfused with cell-free solutions.^{34–36} In contrast, lungs from *MIF*^{-/-} mice demonstrated an increase in PA pressure which was maintained throughout the period of hypoxia (Fig. 2a) reflecting a sustained increase in PVR. We quantified acute hypoxic vasoconstriction in two ways; first, we compared the peak increases in PA pressure observed during the acute hypoxic challenge in *MIF*^{-/-} and *MIF*^{+/+} mice and found that this was very similar in both groups (Fig. 2b). However, the more prolonged, steady state acute hypoxic vasoconstrictor response (i.e. that observed just before the end of the 10 min hypoxic challenge) was significantly greater in *MIF*^{-/-} mice than in the *MIF*^{+/+} mice (Fig. 2c).

Systemic response to sustained hypoxia

MIF deletion did not lead to any change in hematocrit or body weight, under normoxic conditions (Table 1). Following sustained hypoxic exposure (three weeks), both genotypes showed a significant elevation in hematocrit that was very similar. Both genotypes also showed characteristic losses in weight in response to chronic hypoxia.

PVR in chronic hypoxia

Chronic HPH results from increased PVR, since cardiac output remains unchanged following the onset of alveolar hypoxia.³ Thus, to test whether MIF plays a significant role in the development of HPH *in vivo*, we examined PVR in lungs isolated from mice that had been exposed to three weeks of hypoxia. This preparation offered the advantage over measurement of PA pressure *in vivo* (which depends on multiple variables including cardiac output, left atrial pressure and PVR) that it allowed a direct examination of the effects of MIF loss on the pulmonary circulation without any possible confounding effects of changes in cardiac function that might have been induced by MIF deletion.

In lungs isolated from normoxic mice, PVR was very similar in *MIF*^{+/+} and *MIF*^{-/-} animals (Fig. 3a). Chronic hypoxic exposure significantly increased PVR in both genotypes; however, the increase in vascular resistance in *MIF*^{-/-} mice was significantly greater than that observed in *MIF*^{+/+} mice (Fig. 3a). MIF deletion did not cause any change in RV

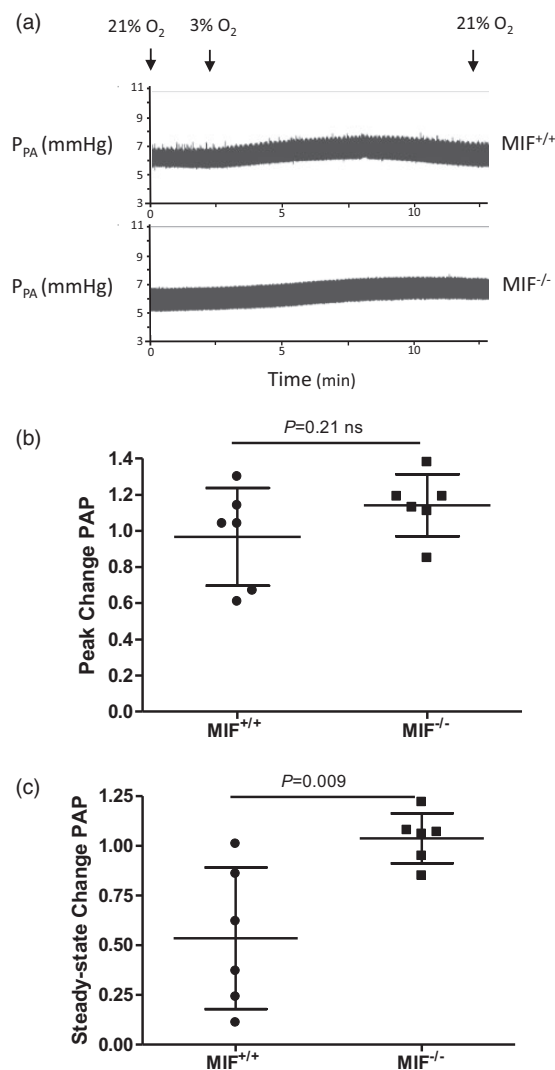


Fig. 2. Changes in PA pressure (PAP) in isolated ventilated perfused lungs in response to acute hypoxic challenge in isolated ventilated perfused lungs. Following stabilization during ventilation with normoxic gas (CO₂ 5% in air), the isolated perfused lung was ventilated with hypoxic gas (O₂ 3%, CO₂ 5%, balance N₂) for 10 min. (a) Reproduction of typical experimental records showing PA pressure, immediately prior to, and during hypoxic challenge, in a *MIF*^{+/+} and a *MIF*^{-/-} mice. (b) Mean (± SD) peak changes in PA pressure during acute hypoxic challenge in *MIF*^{+/+} and *MIF*^{-/-} mice. (c) Mean (± SD) steady-state changes in PA pressure during acute hypoxia challenge in *MIF*^{+/+} and *MIF*^{-/-} mice.

P_{PA}: pulmonary artery pressure; *MIF*^{+/+}: Macrophage migration inhibitory factor wild-type; *MIF*^{-/-}: Macrophage migration inhibitory factor knockout.

size under normoxic conditions. In response to hypoxia, *MIF*^{-/-} mice developed significant right ventricular hypertrophy (RVH), which was very similar to that observed in *MIF*^{+/+} mice (Fig. 3b).

We also examined the responses of MIF haploinsufficient mice (*MIF*^{+/-}) to acute and chronic hypoxia exposure and found that both acute hypoxic vasoconstriction, and the responses to chronic hypoxia were closely similar to those

Table 1. Hematocrit and body weight of mice following sustained hypoxic exposure (three weeks).

	<i>MIF</i> ^{+/+}		<i>MIF</i> ^{-/-}	
	Normoxic (n = 16)	Hypoxic (n = 16)	Normoxic (n = 14)	Hypoxic (n = 18)
Hematocrit (%)	43.0 (3.9)	60.8 (3.1) ^a	43.2 (2.3)	63.5 (4.2) ^a
Entry weight (g)	28.3 (2.3)	28.2 (2.9)	26.8 (1.7)	27.9 (2.2)
Change in weight (%)	6.3 (5.1)	-1.6 (4.4) ^a	5.2 (4.9)	-2.5 (5.7) ^a

MIF^{+/+}: Macrophage migration inhibitory factor wild-type; *MIF*^{-/-}: Macrophage migration inhibitory factor knockout.

Note: Values are mean (SD).

^aSignificantly different from normoxic control group for the same genotype ($P < 0.001$).

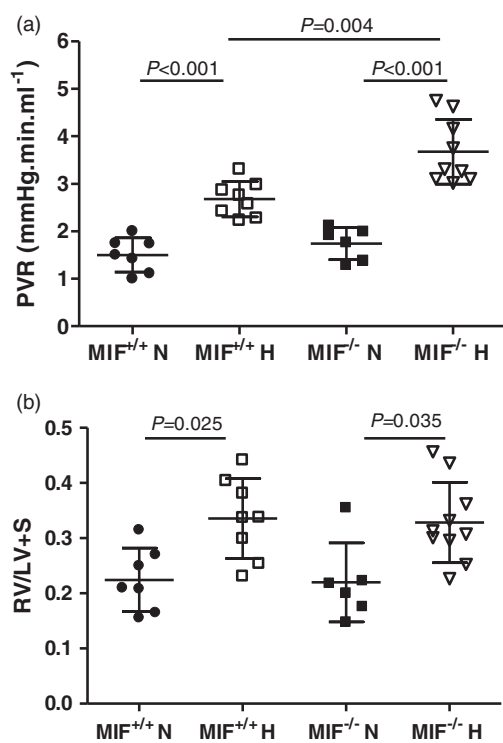


Fig. 3. Pulmonary vascular resistance in isolated ventilated perfused lungs and RV/(LV + S) in normoxic and chronically hypoxic mice. (a) PVR in isolated ventilated perfused lungs from *MIF*^{+/+} and *MIF*^{-/-} groups maintained in normoxia or chronic hypoxia. (b) RV/(LV + S) in *MIF*^{+/+} and *MIF*^{-/-} maintained in normoxia or chronic hypoxia. Values are expressed as mean (\pm SD). P values indicate statistical significance of the difference between groups (unpaired t-test with Holm-Sidak correction). PVR: pulmonary vascular resistance; *MIF*^{+/+}: Macrophage migration inhibitory factor wild-type; *MIF*^{-/-}: Macrophage migration inhibitory factor knockout; RV/(LV + S): ratio of the right ventricle to the left ventricle plus septum.

of *MIF*^{+/+} mice (data not shown). In view of this, the *MIF*^{+/-} mice were excluded from further investigations.

Vasoconstriction independent increase in PVR in chronic hypoxia

In order to assess the magnitude of the increase in PVR that was independent of any hypoxic vasoconstriction in the

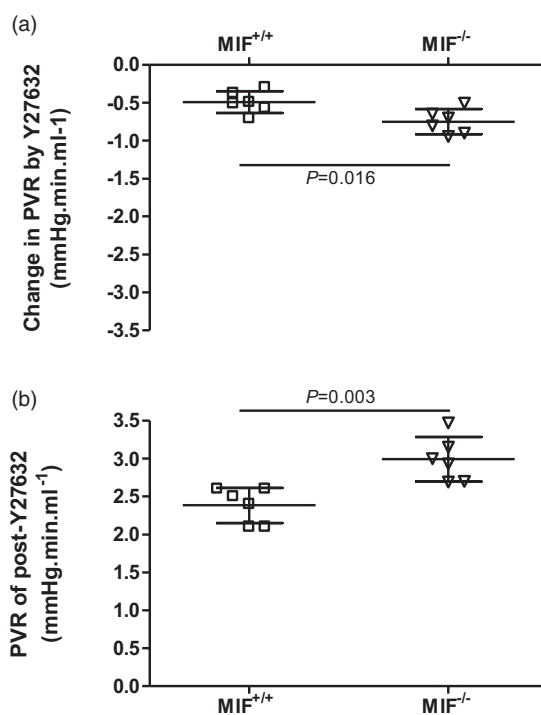


Fig. 4. Vasoconstrictor independent hypoxic vascular resistance in isolated perfused lungs. (a) Reduction in PVR induced by rho kinase inhibition (Y-27632; 10^{-5} M) in chronically hypoxic lungs was significantly greater in *MIF*^{-/-} mice than in *MIF*^{+/+} mice. (b) PVR in chronically hypoxic *MIF*^{-/-} mouse lungs following maximal vasodilation (post Y-27632) remained significantly greater than that in chronically hypoxic *MIF*^{+/+} mouse lungs. Values are expressed as mean (\pm SD). P values indicate statistical significance of the difference between groups (unpaired t-test).

MIF^{+/+}: Macrophage migration inhibitory factor wild-type; *MIF*^{-/-}: Macrophage migration inhibitory factor knockout; PVR: pulmonary vascular resistance.

chronically hypoxic *MIF*^{-/-} mice, we used the potent rho kinase inhibitor Y-27632. At the concentration we used (10^{-5} M), it has been previously shown to completely abolish vasomotor tone in the mouse lung.²⁷ We found that rho kinase inhibition led to a statistically significantly greater vasodilator response in chronically hypoxic lungs from *MIF*^{-/-} mice than in lungs from *MIF*^{+/+} mice (Fig. 4a),

although the magnitude of the difference was relatively small. Importantly, hypoxic PVR remained substantially greater in $MIF^{-/-}$ mice than in the $MIF^{+/+}$ mice after fully relaxing vascular smooth muscle tone (Fig. 4b), suggesting that structural changes in the pulmonary circulation were the predominant factor causing the increased PVR in hypoxic $MIF^{-/-}$ mice.

Structural changes in pulmonary vasculature

To investigate pulmonary vascular remodelling, groups of $MIF^{+/+}$ and $MIF^{-/-}$ mice were exposed to three weeks of hypoxia and their lungs isolated and fixed at standard vascular and airway pressures, following Y-27632-induced vascular relaxation, to allow stereological analysis of changes in pulmonary vascular structure.

In response to three weeks of hypoxia, the walls of the small intra-acinar vessels in the hypoxic groups demonstrated characteristic thickening, which appeared to be similar in $MIF^{+/+}$ and $MIF^{-/-}$ mice (Figs 5 and 6a). We next examined the changes in lumen diameter that occurred in hypoxia, since those are a major determinant of vascular resistance. Although the mean luminal diameters of the small intra-acinar vessels in hypoxic mice were reduced when compared to those in normoxic mice of the same genotype (Fig. 6b), the associated P values did not reach the conventional threshold for statistical significance ($P=0.064$ and $P=0.050$). The total length of the intra-

acinar vessels was not significantly increased by chronic hypoxia in either genotype (Fig. 6c).

We next calculated the ratio of the vascular resistance of the non-capillary, intra-acinar vessels in each lung to that of a standard normoxic lung, i.e. a lung in which the mean luminal diameter and the mean length of those vessels equalled the average values calculated for the wild-type normoxic group. By expressing the mean lumen diameter and total length of vessels in each mouse lung (following maximal vasodilation with rho kinase inhibitor) in that way, we estimated the structural component of the vascular resistance of the non-capillary vessels in each lung relative to the standard normoxic lung using Poiseuille's equation. In both $MIF^{+/+}$ and $MIF^{-/-}$ mice, the calculated structural component of vascular resistance caused by the fully dilated small intra-acinar, non-capillary vessel structure following three weeks of hypoxia was significantly greater than that in the corresponding normoxic controls of the same genotype (Fig. 6d). Moreover, the magnitude of the hypoxia-induced increase in PVR was similar for both genotypes. These findings suggest that, while the structural changes observed in the intra-acinar vessels contributed to the increased PVR in hypoxic groups compared to the normoxic groups of the same genotype, those changes did not account for the difference in PVR between hypoxic $MIF^{+/+}$ and $MIF^{-/-}$ mice that remained during perfusion following maximal vasodilatation with rho kinase inhibitor (Fig. 4).

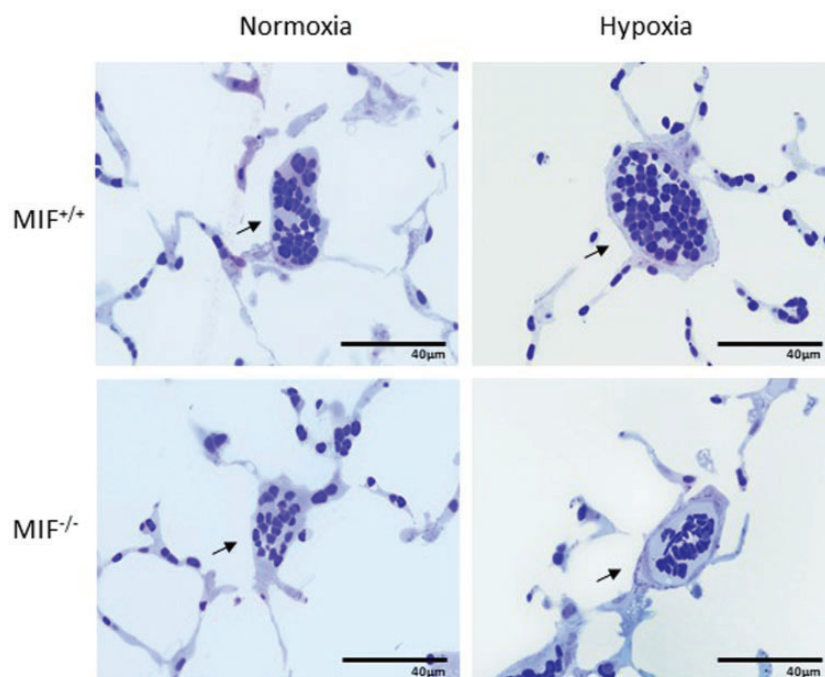


Fig. 5. Microscopic images of pulmonary arterial vessels taken from normoxic and hypoxic lungs of wild-type and MIF knockout mice. Representative images of small intra-acinar vessels (black arrows) in $MIF^{+/+}$ and $MIF^{-/-}$ mice exposed to normoxic and chronically hypoxic conditions ($\times 100$ oil immersion objective, NA 2.1).

$MIF^{+/+}$: Macrophage migration inhibitory factor wild-type; $MIF^{-/-}$: Macrophage migration inhibitory factor knockout.

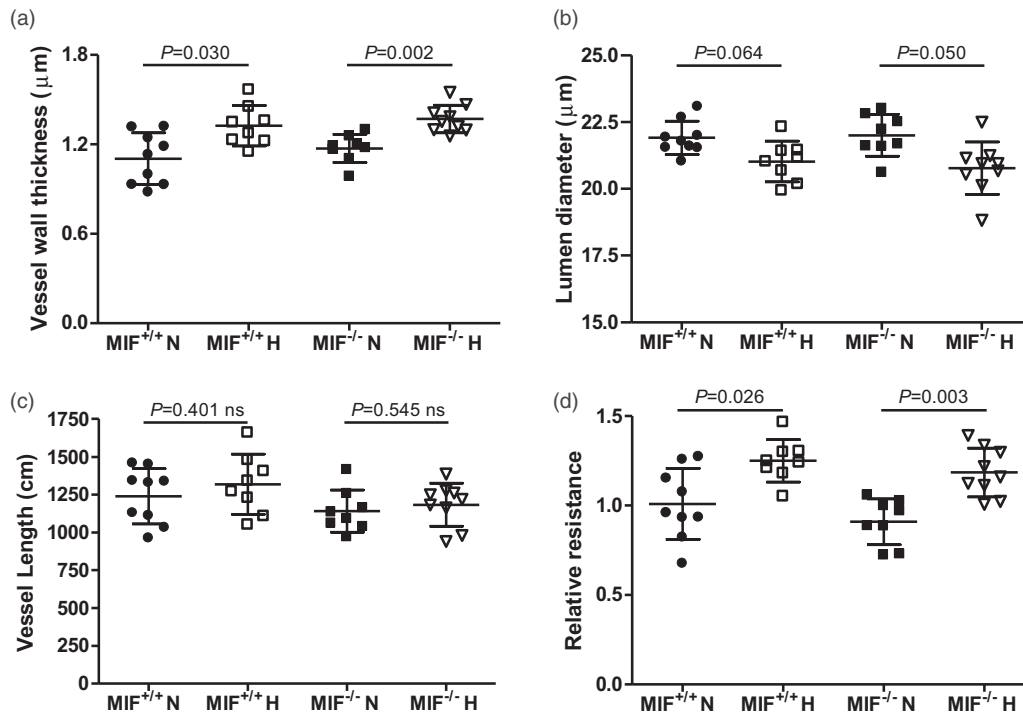


Fig. 6. Dimensions of maximally dilated vessels within the gas exchange regions of the lungs of wild-type and MIF knockout mice. (a) Vessel wall thickness in $MIF^{+/+}$ and $MIF^{-/-}$ in normoxia and chronic hypoxia. (b) Lumen diameter in $MIF^{+/+}$ and $MIF^{-/-}$ mice in normoxia and chronic hypoxia. (c) Total length of intra-acinar vessels in $MIF^{+/+}$ and $MIF^{-/-}$ mice in normoxia and chronic hypoxia. (d) Estimated vascular resistance of the intra-acinar vessels (excluding capillaries) following maximal vasodilatation (structural vascular resistance) which was calculated using Poiseuille's equation and expressed relative to the mean value in the normoxic $MIF^{+/+}$ group (Relative resistance, see text for details). All values are shown as mean (\pm SD). *P* values indicate statistical significance of the difference between groups (unpaired t-test with Holm-Sidak correction). $MIF^{+/+}$: Macrophage migration inhibitory factor wild-type; $MIF^{-/-}$: Macrophage migration inhibitory factor knockout.

Both $MIF^{+/+}$ and $MIF^{-/-}$ mice showed a significant increase in lung volume in response to sustained hypoxia (Fig. 7a) when inflated at standard airway pressure. Total epithelial surface area was increased significantly in $MIF^{+/+}$ mice in response to chronic hypoxia when compared to normoxic $MIF^{+/+}$ mice (Fig. 7b) and was accompanied by a corresponding increase in capillary endothelial surface area (Fig. 7c). However, an hypoxia-induced increase was not observed in $MIF^{-/-}$ mice when compared to both normoxic $MIF^{-/-}$ and $MIF^{+/+}$ mice, resulting in a significantly smaller total epithelial and endothelial surface area in hypoxic $MIF^{-/-}$ mice compared to that in hypoxic $MIF^{+/+}$ mice (Fig. 7b and c). Taken together, these data indicate that in response to chronic hypoxia, $MIF^{-/-}$ mice did not expand their total alveolar capillary bed, in contrast to the marked expansion observed in hypoxic wild types. Thus, a failure to expand the pulmonary capillary bed may have caused the greater structural increase in PVR observed in chronically hypoxic $MIF^{-/-}$ mice.

Role of MIF in pulmonary endothelial apoptosis

Given the reduced vascular bed in the $MIF^{-/-}$ mouse lungs, we examined the action of MIF on pulmonary microvascular endothelial cells in vitro. HPMECs were initially grown

to 70% confluence in full growth medium (GM), i.e. BM to which all growth factors had been added. Following this, the cells were grown for a further 24h in one of the following four conditions: complete GM, i.e. BM with all growth factors included, BM alone (i.e. omission of all growth factors) to provoke apoptosis, BM with recombinant human VEGF added or BM with recombinant human MIF (rMIF) added. Following growth in these conditions, caspase 3/7 activity was assayed as an index of apoptosis (Fig. 8). The results showed that removal of all growth factors in HPMECs resulted in a significant increase in endothelial apoptosis (Fig. 8). Restoration of VEGF alone reduced apoptosis to basal levels confirming its central anti-apoptotic role in pulmonary microvascular endothelial cells.³⁷ Addition of rMIF also significantly inhibited apoptosis (Fig. 8). It is worth noting that the anti-apoptotic action of MIF was almost as effective as that of VEGF. These results indicate that in the absence of MIF, human endothelial cells exhibit increased caspase 3/7 activities, leading to an increase in endothelial cell apoptosis.

Discussion

The novel findings of our study indicate that complete MIF deficiency caused a greater increase in PVR in response to

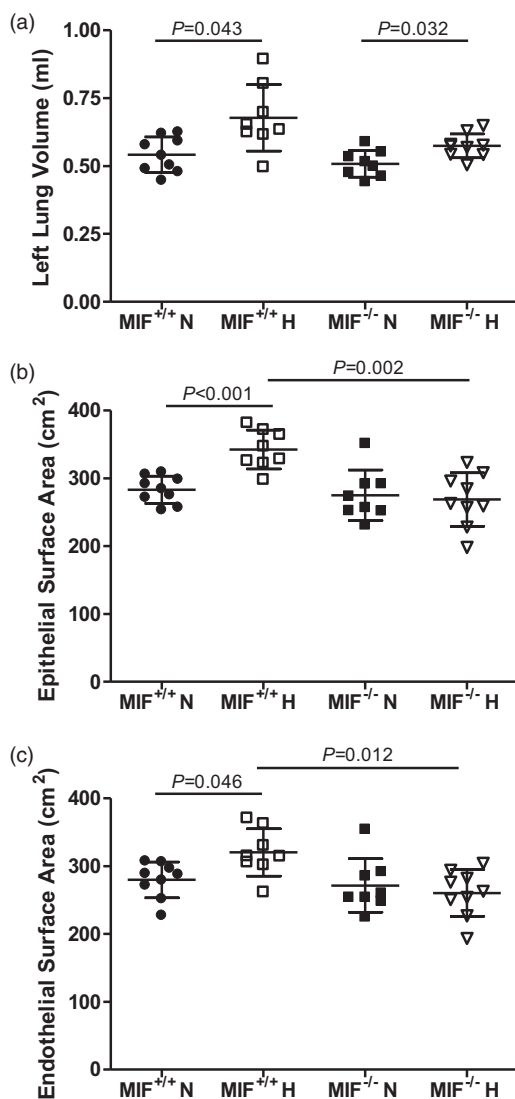


Fig. 7. Left lung volumes, total left lung epithelial and endothelial surface areas. (a) Lung volumes in both $MIF^{+/+}$ and $MIF^{-/-}$ mice. (b) Total epithelial surface area in the left lungs of $MIF^{+/+}$ mice and $MIF^{-/-}$ mice. (c) Total endothelial surface area in the left lungs of $MIF^{+/+}$ mice and $MIF^{-/-}$ mice. All values are shown as mean (\pm SD). P values indicate statistical significance of the difference between groups (unpaired t-test with Holm-Sidak correction). $MIF^{+/+}$: Macrophage migration inhibitory factor wild-type; $MIF^{-/-}$: Macrophage migration inhibitory factor knockout.

chronic alveolar hypoxia than that observed in chronically hypoxic wild-type mice. Interestingly, the increased vascular resistance in hypoxic $MIF^{-/-}$ mice was not due to greater remodelling of small pulmonary vessels (arterioles and venules), which was similar to that seen in wild-type mice. Loss of MIF resulted in a smaller pulmonary capillary bed following chronic hypoxic exposure than that in chronically hypoxic wild-type mice. These results collectively suggest that the normal role of MIF during chronic alveolar hypoxia, acting through all its signalling pathways, is to attenuate the development of increased PVR.

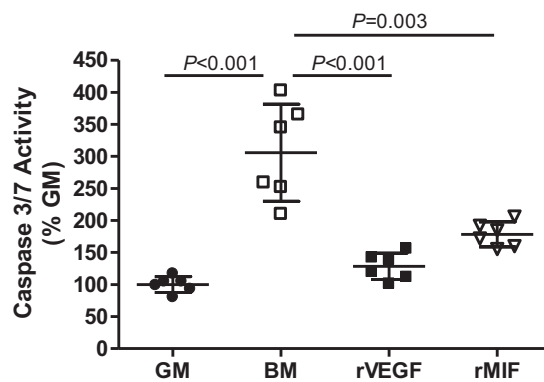


Fig. 8. Caspase 3/7 activity in HPMECs. Caspase 3/7 activity in HPMECs treated with full growth media (GM), basal media (BM), rMIF and rVEGF, respectively. All values are shown as mean (\pm SD). P values indicate statistical significance of the difference between groups (paired t-test with Holm-Sidak correction). rMIF: recombinant human macrophage migration inhibitory factor; rVEGF: recombinant human vascular endothelial growth factor.

Although the $MIF^{-/-}$ mice did not demonstrate any obvious phenotypic abnormalities in the absence of an hypoxic challenge, as previously reported,³⁸ their acute pulmonary vasoconstrictor response to hypoxia was greater than that in the lungs of $MIF^{+/+}$ mice (Fig. 2) suggesting that developmental loss of MIF caused more prolonged acute hypoxic vasoconstriction, even though normoxic (unchallenged) vascular resistance was not different in the two genotypes (Fig. 3a).

We also found that the $MIF^{-/-}$ mice showed greater increases in PVR in response to chronic hypoxia than wild-type mice (Fig. 3a). Most of the increase in PVR was due to structural differences between the pulmonary vascular beds of the two genotypes and not due to increased chronic hypoxic vasoconstriction (Fig. 4). However, the augmented structural component of the vascular resistance following MIF deletion was not due to greater remodelling of the non-capillary vessels within the lungs (arterioles and venules), since this was similar in both genotypes (Fig. 6). Such dissociation of changes in PVR from changes in vascular wall remodelling has previously been reported. For example, chronically hypoxic Protein kinase C (PKC) epsilon-deficient mice showed greater pulmonary arterial pressure than wild-type hypoxic mice but a closely similar muscularization of the pulmonary vessels.³⁹ Similarly, peroxisome proliferator-activated receptor (PPAR) gamma inhibition using rosiglitazone completely blocked pulmonary vascular remodelling without any effect on the elevation of PVR in chronically hypoxic rats.⁴⁰

Prompted by these observations, we sought an alternative structural reason for the increased PVR in the hypoxic $MIF^{-/-}$ mice. Reduction of the pulmonary vascular bed, such as that occurring in chronic obstructive pulmonary disease (COPD) and emphysema, contributes significantly

to increased PVR and the development of PH.^{41–43} We observed a failure of the expansion of the capillary bed in *MIF*^{-/-} lungs (Fig. 7) that is normally seen in wild-type lungs in response to chronic hypoxia.^{27,28,30,44,45} Thus, our data suggest that MIF normally acts to attenuate the increase in PVR in the chronically hypoxic lung by stimulating an expansion of the alveolar capillary network.

Our finding that MIF inhibits apoptosis in HPMECs induced by VEGF withdrawal in vitro (Fig. 8) supports the demonstration that MIF depletion in the mouse causes failure of the normal expansion of the pulmonary capillary bed in response to hypoxia in vivo. It has previously been shown that MIF inhibits apoptosis in pulmonary endothelial cells caused by cigarette smoke^{46–48} and our results are compatible with those previous reports. However, our results extend those previous reports by demonstrating that MIF protects against apoptosis induced by VEGF and growth factor withdrawal. Moreover, MIF is as effective as VEGF in preventing such apoptosis under these conditions. This finding is particularly important given the evidence that inhibition of the VEGF signalling axis plays an important role in the development of PH and emphysema in COPD.^{49–52} Further evidence demonstrating a central role for MIF in maintaining the normal pulmonary capillary bed is provided by the recent demonstration that subjects with the CATT₅ allele, a MIF promoter polymorphism that causes reduced MIF concentrations, have a reduced pulmonary carbon monoxide diffusing capacity, when compared to COPD patients with higher expressing MIF polymorphisms.⁵³ Taken together with these previous reports, our results indicate an important protective role for MIF in the pulmonary capillary circulation exposed to chronic alveolar hypoxia.

It is interesting to note that RVH was not worsened in the hypoxic *MIF*^{-/-} mice despite their significantly greater increase in PVR. Dissociation of the magnitude of RVH from an increase in RV loading has been reported previously by others in different models. For example, it has been shown that in smooth muscle-specific *HIF1alpha*^{-/-} mice HPH was reduced compared to wild-type animals but that RVH was identical in both groups.⁵⁴ A second example of such dissociation is provided by the work of Yet et al. who showed that, while PA pressure was reduced in chronically hypoxic haem oxygenase-deficient (*HO*^{-/-}) mice compared to hypoxic wild-types, RVH was greater in the *HO*^{-/-} mice.⁵⁵ Conversely, rosiglitazone treatment of chronically hypoxic mice reduced RVH without attenuating the increase in PVR.⁴⁰ Further evidence of greater RV load without a corresponding increase in RVH is provided by the work of Bogaard and colleagues.⁵⁶ They produced chronic RV overload in rats by banding of the PA so that RV pressure was increased to the same extent as in a group of mice subjected to the Sugen-hypoxia model of PH. Six weeks later, RVH was very substantially less in the banded group.⁵⁶ Thus, previous reports have shown that the magnitude of RVH is not directly or uniquely related to an increased PA pressure caused by increased vascular resistance in mice and rats.⁵⁷

An alternative potential mechanism that could account for the absence of greater RVH in the presence of a greater increase in PVR in the hypoxic *MIF*^{-/-} mice must be considered, i.e. that PA pressure did not increase in vivo. Since all of the cardiac output must pass through the pulmonary circulation and the PVR was increased in hypoxic *MIF*^{-/-} mice compared to *MIF*^{+/+} mice, a reduction in cardiac output could have maintained similar pulmonary arterial pressure in both mouse genotypes and thus kept the load on the right ventricle similar in both groups. We cannot definitively exclude an unchanged RV load in the chronically *MIF*^{-/-} mice compared to the chronically hypoxic *MIF*^{+/+} mice as we did not measure pulmonary arterial pressure in vivo.

While the present study shows that genetic deletion of MIF leads to worsening of the hypoxia-induced increase in PVR, it is important to note that it has been previously reported that two other, different, approaches to inhibiting MIF activity partially protected against the development of PH in rodents in vivo.^{9,10} MIF tautomerase inhibitors attenuate the development of PH caused by chronic hypoxia or MCT and anti-CD74 neutralizing antibodies attenuated the development of MCT-induced PH.^{9,10} How might these divergent results be explained?

The first potential reason for the difference between the augmented pulmonary resistance in hypoxic *MIF*^{-/-} mice that we observed and the protective effects of the tautomerase inhibitors observed by others is that MIF has multiple mechanisms of action, not all of which are blocked by the tautomerase inhibitors. MIF signals through at least three cell surface receptors, including the CD74/44 complex, CXCR2 and CXCR4^{16–18} but also signals by intracellular interaction with the JAB-1 thus inhibiting JNK activation and p27^{Kip1}-dependent cell-cycle regulation.^{19,20} The exact inhibitory mechanisms of the MIF tautomerase inhibitors ISO-1 and its analogues remain to be fully investigated. There is evidence of their physically blocking MIF-CD74 interactions in vitro^{11–15} and of an inhibitory effect on MIF-CXCR4 interaction in vitro.⁵⁸ However, the effect of MIF tautomerase inhibitors on the other MIF-signalling pathways is unknown and their activities in vivo remain to be fully elucidated, particularly in the context of lung disease. Thus, treatment with ISO-1 or anti-CD74 neutralizing antibodies does not block all MIF functions completely in vivo and would not produce effects identical to the permanent loss of all MIF functions that occurs in the *MIF*^{-/-} mice. It is important to note that divergent actions of genetic MIF deletion and inhibition of MIF with ISO-1, similar to those we report here, have previously been reported in the lung by others. Genetic deletion of MIF worsened cigarette smoke-induced lung damage in mice,⁵⁹ whereas inhibition of MIF by ISO-1 ameliorated ozone-induced lung damage in mice, a model of COPD-associated oxidant stress.⁶⁰ Taken together with our results, this suggests that in certain contexts, the normal effect of all MIF functions acting in concert at normal levels is protective and homeostatic.

A second possible reason for differences between the effects of pharmacological inhibition of MIF tautomerase activity and complete genetic deletion of MIF is that ISO-1 and similar compounds may not completely inhibit MIF binding to CD74 at the doses used in vivo. Thus such agents at lower doses may reduce MIF activity but not abolish it completely permitting retention of some essential homeostatic functions while preventing the damaging effects of excessive MIF concentrations. Pharmacological inhibitors may also have actions that are beneficial but not mediated by inhibition of MIF. For example, ISO-1 may block the actions of other cytokines that share structurally similar sites such as D-dopachrome tautomerase.⁶¹

A further important difference between *MIF*^{-/-} mice and the use of inhibitors of MIF actions is that in the genetically modified mouse *MIF* expression is absent throughout development. This may have caused subtle changes in lung vascular structure or function that were not detectable under normal conditions but which made the lung more vulnerable to the development of increased PVR when challenged by sustained hypoxia in adulthood. Support for this possibility is provided by our observation of increased expression of IL-6 and vascular cell adhesion molecule (VCAM)-1 in the unchallenged normoxic lungs of *MIF*^{-/-} mice at three months of age (data not shown), and our finding that acute hypoxic pulmonary vasoconstriction was also increased in these mice (Fig. 2), even though there were no detectable structural abnormalities or changes in PVR at that time (Figs 3, 6 and 7). Others have previously reported developmental delay in the lungs of embryonic and perinatal *MIF*^{-/-} mice, which is also compatible with subtle developmental differences making the lung more vulnerable to the effects of chronic alveolar hypoxia on the pulmonary circulation later in life.^{62,63}

The complexity of MIF biology in the context of hypoxic pulmonary diseases is also reflected in the results of clinical studies. Increased concentrations of MIF compared to healthy controls have been reported in the serum of sputum of patients with COPD in some studies, with further increases during acute exacerbations.^{60,64} In contrast, others have reported reduced serum MIF in COPD with the lowest concentrations observed in the most severe (GOLD IV) disease.⁴⁸ Furthermore, a MIF polymorphism that causes reduced MIF expression is associated with reduced diffusing capacity for carbon monoxide in COPD patients.⁵³ Similarly, in patients with community-acquired pneumonia, lower expressing MIF polymorphisms are associated with increased risk of systemic sepsis and 90-day mortality.⁶⁵ However, in contrast to those studies linking reduced MIF expression to poorer clinical outcomes, cystic fibrosis patients with MIF promoter polymorphisms that cause lower levels of MIF expression are at reduced risk of *Pseudomonas aeruginosa* infection and organ damage when compared to patients with highly expressing polymorphisms.⁶⁶ Thus the roles of MIF in lung diseases remain unclear and further work is required to elucidate these.

Taken together with our data showing a greater increase in PVR in chronically hypoxic mice following complete loss of MIF, these contrasting reports and uncertainties suggest that caution must be exercised in translating MIF blocking strategies into clinical use. It may be important to avoid complete blockade of all MIF functions and to block only certain actions of this pleiotropic cytokine to achieve a beneficial therapeutic effect. This may in fact be one of the benefits of using MIF tautomerase inhibitors, such as ISO-1, as at the right dose they may block the deleterious pro-inflammatory effects of MIF without affecting the homeostatic or protective actions.

It is important to note that we used male mice in all experiments and that the endothelial cells used in the in vitro studies were from a male donor. There are important sex differences in PH and the mechanisms of these remain incompletely understood.^{67,68} Therefore, when designing our experiments, we used male mice so that any differences seen could be attributed to the effects of MIF deletion on the hypoxic responses without any confounding effects of sex-based differences. In view of this, further work will be required to determine whether MIF plays the same role in the hypoxic female lung. Until such work is completed, caution must be exercised before extrapolating the implications of our findings from males to females.

In conclusion, we found that *MIF*^{-/-} mice developed a greater increase in PVR than wild-type mice during sustained exposure to hypoxia as a consequence of both increased pulmonary vasoconstriction and a reduced alveolar capillary bed. These findings demonstrate an important protective and homeostatic role for MIF in the pulmonary circulation and suggest that complete loss of all MIF functions may be detrimental in the hypoxic lung.

Acknowledgments

Grateful thanks to Prof Jürgen Bernhagen for providing us the initial MIF knockout mice and Dr Daniel Crean for his advice on the caspase assay.

Funding

Science Foundation Ireland (RFP MIMF306 – JB, 12/IA/1477 – PMcL).

Ethical approval


Approved by the UCD Animal Research Ethics Committee.

Author contributions

P.Mc.L. and J.B. contributed to study design, data analysis, and paper writing; S.C.R., K.H. and S.C.D. contributed to study design and paper review; and L.L., M.X. and A.R.-H. contributed to data acquisition, data analysis and paper writing/review.

Conflict of interest

The author(s) declare that there is no conflict of interest.

ORCID iDsLili Li  <https://orcid.org/0000-0002-1888-4604>Simon C. Rowan  <https://orcid.org/0000-0002-4103-4421>**Supplemental Material**

Supplemental material for this article is available online

References

- Seeger W, Adir Y, Barbera JA, et al. Pulmonary hypertension in chronic lung diseases. *J Am Coll Cardiol* 2013; 62: D109–D116. Research Support, Non-U.S. Gov't.
- Rowan SC, Keane MP, Gaine S, et al. Hypoxic pulmonary hypertension in chronic lung diseases: novel vasoconstrictor pathways. *Lancet Respir Med* 2016; 4: 225–236.
- Groves BM, Reeves JT, Sutton JR, et al. Operation Everest II: elevated high-altitude pulmonary resistance unresponsive to oxygen. *J Appl Physiol (1985)* 1987; 63: 521–530.
- West JB. The physiologic basis of high-altitude diseases. *Ann Intern Med* 2004; 141: 789–800.
- Nathan SD, Barbera JA, Gaine SP, et al. Pulmonary hypertension in chronic lung disease and hypoxia. *Eur Respir J* 2019; 53: 1801914.
- Wilkins MR, Ghofrani HA, Weissmann N, et al. Pathophysiology and treatment of high-altitude pulmonary vascular disease. *Circulation* 2015; 131: 582–590.
- Baugh JA, Gantier M, Li L, et al. Dual regulation of macrophage migration inhibitory factor (MIF) expression in hypoxia by CREB and HIF-1. *Biochem Biophys Res Commun* 2006; 347: 895–903.
- Jalce G and Guignabert C. The multiple roles of macrophage migration inhibitory factor in pulmonary hypertension. *Am J Physiol Lung Cell Mol Physiol* 2020; 318: L1–L9.
- Zhang Y, Talwar A, Tsang D, et al. Macrophage migration inhibitory factor mediates hypoxia-induced pulmonary hypertension. *Mol Med* 2012; 18: 215–223.
- Le Hirsch M, Tu L, Ricard N, et al. Proinflammatory signature of the dysfunctional endothelium in pulmonary hypertension. Role of the macrophage migration inhibitory factor/CD74 complex. *Am J Respir Crit Care Med* 2015; 192: 983–997.
- Leng L, Chen L, Fan J, et al. A small-molecule macrophage migration inhibitory factor antagonist protects against glomerulonephritis in lupus-prone NZB/NZW F1 and MRL/lpr mice. *J Immunol* 2011; 186: 527–538.
- Jorgensen WL, Trofimov A, Du X, et al. Benzisothiazolones as modulators of macrophage migration inhibitory factor. *Bioorg Med Chem Lett* 2011; 21: 4545–4549.
- Stamps SL, Taylor AB, Wang SC, et al. Mechanism of the phenylpyruvate tautomerase activity of macrophage migration inhibitory factor: properties of the P1G, P1A, Y95F, and N97A mutants. *Biochemistry* 2000; 39: 9671–9678.
- Lubetsky JB, Swope M, Dealwis C, et al. Pro-1 of macrophage migration inhibitory factor functions as a catalytic base in the phenylpyruvate tautomerase activity. *Biochemistry* 1999; 38: 7346–7354.
- Bendrat K, Al-Abed Y, Callaway DJ, et al. Biochemical and mutational investigations of the enzymatic activity of macrophage migration inhibitory factor. *Biochemistry* 1997; 36: 15356–15362.
- Leng L, Metz CN, Fang Y, et al. MIF signal transduction initiated by binding to CD74. *J Exp Med* 2003; 197: 1467–1476.
- Shi X, Leng L, Wang T, et al. CD44 is the signaling component of the macrophage migration inhibitory factor-CD74 receptor complex. *Immunity* 2006; 25: 595–606.
- Bernhagen J, Krohn R, Lue H, et al. MIF is a noncognate ligand of CXC chemokine receptors in inflammatory and atherogenic cell recruitment. *Nat Med* 2007; 13: 587–596.
- Kleemann R, Hausser A, Geiger G, et al. Intracellular action of the cytokine MIF to modulate AP-1 activity and the cell cycle through Jab1. *Nature* 2000; 408: 211–216.
- Luedike P, Hendgen-Cotta UB, Sobierajski J, et al. Cardioprotection through S-nitros(yl)ation of macrophage migration inhibitory factor. *Circulation* 2012; 125: 1880–1889.
- Israelson A, Ditsworth D, Sun S, et al. Macrophage migration inhibitory factor as a chaperone inhibiting accumulation of misfolded SOD1. *Neuron* 2015; 86: 218–232.
- Nguyen MT, Lue H, Kleemann R, et al. The cytokine macrophage migration inhibitory factor reduces pro-oxidative stress-induced apoptosis. *J Immunol* 2003; 170: 3337–3347.
- Rosengren E, Bucala R, Aman P, et al. The immunoregulatory mediator macrophage migration inhibitory factor (MIF) catalyzes a tautomerization reaction. *Mol Med* 1996; 2: 143–149.
- Sugimoto H, Taniguchi M, Nakagawa A, et al. Crystal structure of human D-dopachrome tautomerase, a homologue of macrophage migration inhibitory factor, at 1.54 Å resolution. *Biochemistry* 1999; 38: 3268–3279.
- Fingerle-Rowson G, Petrenko O, Metz CN, et al. The p53-dependent effects of macrophage migration inhibitory factor revealed by gene targeting. *Proc Natl Acad Sci U S A* 2003; 100: 9354–9359.
- Howell K, Preston RJ and McLoughlin P. Chronic hypoxia causes angiogenesis in addition to remodelling in the adult rat pulmonary circulation. *J Physiol* 2003; 547: 133–145.
- Cahill E, Rowan SC, Sands M, et al. The pathophysiological basis of chronic hypoxic pulmonary hypertension in the mouse: vasoconstrictor and structural mechanisms contribute equally. *Exp Physiol* 2012; 97: 796–806.
- Cahill E, Costello CM, Rowan SC, et al. Gremlin plays a key role in the pathogenesis of pulmonary hypertension. *Circulation* 2012; 125: 920–930.
- Li L, Howell K, Sands M, et al. The alpha and Delta isoforms of CREB1 are required to maintain normal pulmonary vascular resistance. *PloS One* 2013; 8: e80637.
- Hyvelin JM, Howell K, Nichol A, et al. Inhibition of Rho-kinase attenuates hypoxia-induced angiogenesis in the pulmonary circulation. *Circ Res* 2005; 97: 185–191.
- Howell K, Costello CM, Sands M, et al. L-Arginine promotes angiogenesis in the chronically hypoxic lung: a novel mechanism ameliorating pulmonary hypertension. *Am J Physiol Lung Cell Mol Physiol* 2009; 296: L1042–L1050.
- Hsia CC, Hyde DM, Ochs M, et al. An official research policy statement of the American Thoracic Society/European Respiratory Society: standards for quantitative assessment of lung structure. *Am J Respir Crit Care Med* 2010; 181: 394–418.
- Ludbrook J. Multiple comparison procedures updated. *Clin Exp Pharmacol Physiol* 1998; 25: 1032–1037.

34. Weissmann N, Akkayagil E, Quanz K, et al. Basic features of hypoxic pulmonary vasoconstriction in mice. *Respir Physiol Neurobiol* 2004; 139: 191–202.
35. Murtaza G, Mermer P, Goldenberg A, et al. TASK-1 potassium channel is not critically involved in mediating hypoxic pulmonary vasoconstriction of murine intra-pulmonary arteries. *PLoS One* 2017; 12: e0174071.
36. Yoo HY, Zeifman A, Ko EA, et al. Optimization of isolated perfused/ventilated mouse lung to study hypoxic pulmonary vasoconstriction. *Pulm Circ* 2013; 3: 396–405.
37. Sakao S, Tatsumi K and Voelkel NF. Endothelial cells and pulmonary arterial hypertension: apoptosis, proliferation, interaction and transdifferentiation. *Respir Res* 2009; 10: 95.
38. Bozza M, Satoskar AR, Lin G, et al. Targeted disruption of migration inhibitory factor gene reveals its critical role in sepsis. *J Exp Med* 1999; 189: 341–346.
39. Littler CM, Wehling CA, Wick MJ, et al. Divergent contractile and structural responses of the murine PKC-epsilon null pulmonary circulation to chronic hypoxia. *Am J Physiol Lung Cell Mol Physiol* 2005; 289: L1083–L1093.
40. Crossno JT Jr, Garat CV, Reusch JE, et al. Rosiglitazone attenuates hypoxia-induced pulmonary arterial remodeling. *Am J Physiol Lung Cell Mol Physiol* 2007; 292: L885–L897.
41. Bunel V, Guyard A, Dauriat G, et al. Pulmonary arterial histologic lesions in patients with COPD with severe pulmonary hypertension. *Chest* 2019; 156: 33–44.
42. Washko GR, Nardelli P, Ash SY, et al. Arterial vascular pruning, right ventricular size, and clinical outcomes in chronic obstructive pulmonary disease. A longitudinal observational study. *Am J Respir Crit Care Med* 2019; 200: 454–461.
43. Weatherald J, Montani D and Humbert M. Seeing the forest for the (Arterial) tree: vascular pruning and the chronic obstructive pulmonary disease pulmonary vascular phenotype. *Am J Respir Crit Care Med* 2019; 200: 406–408.
44. Nishimura R, Nishiwaki T, Kawasaki T, et al. Hypoxia-induced proliferation of tissue-resident endothelial progenitor cells in the lung. *Am J Physiol Lung Cell Mol Physiol* 2015; 308: L746–L758.
45. Yilmaz C, Ravikumar P, Gyawali D, et al. Alveolar-capillary adaptation to chronic hypoxia in the fatty lung. *Acta Physiol* 2015; 213: 933–946.
46. Fallica J, Varela L, Johnston L, et al. Macrophage migration inhibitory factor: a novel inhibitor of apoptosis signal-regulating kinase 1-p38-xanthine oxidoreductase-dependent cigarette smoke-induced apoptosis. *Am J Respir Cell Mol Biol* 2016; 54: 504–514.
47. Damico R, Simms T, Kim BS, et al. p53 mediates cigarette smoke-induced apoptosis of pulmonary endothelial cells: inhibitory effects of macrophage migration inhibitor factor. *Am J Respir Cell Mol Biol* 2011; 44: 323–332.
48. Fallica J, Boyer L, Kim B, et al. Macrophage migration inhibitory factor is a novel determinant of cigarette smoke-induced lung damage. *Am J Respir Cell Mol Biol* 2014; 51: 94–103.
49. Voelkel NF and Gomez-Arroyo J. The role of vascular endothelial growth factor in pulmonary arterial hypertension. The angiogenesis paradox. *Am J Respir Cell Mol Biol* 2014; 51: 474–484.
50. Le A, Zielinski R, He C, et al. Pulmonary epithelial neuropilin-1 deletion enhances development of cigarette smoke-induced emphysema. *Am J Respir Crit Care Med* 2009; 180: 396–406.
51. Petrache I, Natarajan V, Zhen L, et al. Ceramide upregulation causes pulmonary cell apoptosis and emphysema-like disease in mice. *Nat Med* 2005; 11: 491–498.
52. Kasahara Y, Tuder RM, Taraseviciene-Stewart L, et al. Inhibition of VEGF receptors causes lung cell apoptosis and emphysema. *J Clin Invest* 2000; 106: 1311–1319.
53. Zhang C, Ramsey C, Berical A, et al. A functional macrophage migration inhibitory factor promoter polymorphism is associated with reduced diffusing capacity. *Am J Physiol Lung Cell Mol Physiol* 2019; 316: L400–L405.
54. Ball MK, Waypa GB, Mungai PT, et al. Regulation of hypoxia-induced pulmonary hypertension by vascular smooth muscle hypoxia-inducible factor-1alpha. *Am J Respir Crit Care Med* 2014; 189: 314–324.
55. Yet SF, Perrella MA, Layne MD, et al. Hypoxia induces severe right ventricular dilatation and infarction in heme oxygenase-1 null mice. *J Clin Invest* 1999; 103: R23–R29.
56. Bogaard HJ, Natarajan R, Henderson SC, et al. Chronic pulmonary artery pressure elevation is insufficient to explain right heart failure. *Circulation* 2009; 120: 1951–1960.
57. Gomez-Arroyo J, Saleem SJ, Mizuno S, et al. A brief overview of mouse models of pulmonary arterial hypertension: problems and prospects. *Am J Physiol Lung Cell Mol Physiol* 2012; 302: L977–L991.
58. Rajasekaran D, Groning S, Schmitz C, et al. Macrophage migration inhibitory factor-CXCR4 receptor interactions: evidence for partial allosteric agonism in comparison to CXCL₁₂ chemokine. *J Biol Chem* 2016; 291: 15881–15895.
59. Sauler M, Leng L, Trentalange M, et al. Macrophage migration inhibitory factor deficiency in chronic obstructive pulmonary disease. *Am J Physiol Lung Cell Mol Physiol* 2014; 306: L487–L496.
60. Russell KE, Chung KF, Clarke CJ, et al. The MIF antagonist ISO-1 attenuates corticosteroid-insensitive inflammation and airways hyperresponsiveness in an ozone-induced model of COPD. *PLoS One* 2016; 11: e0146102.
61. Merk M, Mitchell RA, Endres S, et al. D-dopachrome tautomerase (D-DT or MIF-2): doubling the MIF cytokine family. *Cytokine* 2012; 59: 10–17.
62. Kevill KA, Bhandari V, Kettunen M, et al. A role for macrophage migration inhibitory factor in the neonatal respiratory distress syndrome. *J Immunol* 2008; 180: 601–608.
63. Sun H, Choo-Wing R, Sureshbabu A, et al. A critical regulatory role for macrophage migration inhibitory factor in hyperoxia-induced injury in the developing murine lung. *PLoS One* 2013; 8: e60560.
64. Husebo GR, Bakke PS, Gronseth R, et al. Macrophage migration inhibitory factor, a role in COPD. *Am J Physiol Lung Cell Mol Physiol* 2016; 311: L1–L7.
65. Yende S, Angus DC, Kong L, et al. The influence of macrophage migration inhibitory factor gene polymorphisms on outcome from community-acquired pneumonia. *FASEB J* 2009; 23: 2403–2411.
66. Plant BJ, Gallagher CG, Bucala R, et al. Cystic fibrosis, disease severity, and a macrophage migration inhibitory factor polymorphism. *Am J Respir Crit Care Med* 2005; 172: 1412–1415.
67. Austin ED, Lahm T, West J, et al. Gender, sex hormones and pulmonary hypertension. *Pulm Circ* 2013; 3: 294–314.
68. Lahm T. Sex differences in pulmonary hypertension: are we cleaning up the mess? *Eur Respir J* 2016; 47: 390–393.